CONF-960994--3

SAND96-0870C
SAND--96-0870C

Metal gettering by boron-silicide precipitates in boron-implanted silicon

S. M. Myers, G. A. Petersen, T. J. Headley, J. R. Michael, T. A. Aselage, and C. H. Seager

Sandia National Laboratories, Albuquerque, New Mexico 87185-1056

RECEIVED
SEP 18 1996
OSTI

Abstract

We show that Fe, Co, Cu, and Au impurities in Si are strongly gettered to boron-silicide precipitates formed by supersaturation B implantation and annealing. Effective binding free energies relative to interstitial solution range from somewhat above 1 to more than 2 eV. The B-Si precipitates formed at temperatures ≤1100°C lack long range structural order but closely resemble the icoashedral B_3Si phase in composition, local bonding, and chemical potential. Evidence indicates that the metal atoms go into solution in the B-Si phase, and this is interpreted in terms of the novel bonding and structural characteristics of B-rich icosahedral compounds.

1. Introduction

Increasingly stringent limits on transition-metal impurities in Si [1] motivate efforts to identify and understand new mechanisms for impurity gettering that act by the segregation of metal atoms to pre-existing low-energy sites, rather than by metal-silicide precipitation, and that are characterized by large binding energies [2,3]. The first of these properties implies that the sinks remain active for arbitrarily small metal concentrations instead of ceasing to operate below a characteristic solid solubility, so that gettering can take place at the extremely low impurity levels projected for future Si devices. The second property means that the impurity sites at the sinks are highly populated relative to solution sites within the Si matrix even at elevated temperatures. A third desirable property of gettering sinks is for them to be compatible with location on the device side rather than the back side of the wafer, enabling smaller diffusion lengths for the accommodation of lower processing temperatures.

In the present article we report studies of a new type of gettering sink satisfying the above criteria: boron-silicide precipitates formed by supersaturation B implantation and annealing. Composition profiling by secondary-ion mass spectrometer (SIMS) demonstrates that Cu, Au, Cu, and Fe segregate from the Si phase to the B-Si precipitates. The microstructure and

DISTRIBUTION OF THIS DOCUMENT IS UNLIMITED

MASTER

DISCLAIMER

Portions of this document may be illegible in electronic image products. Images are produced from the best available original document.

DISCLAIMER

This report was prepared as an account of work sponsored by an agency of the United States Government. Neither the United States Government nor any agency thereof, nor any of their employees, makes any warranty, express or implied, or assumes any legal liability or responsibility for the accuracy, completeness, or usefulness of any information, apparatus, product, or process disclosed, or represents that its use would not infringe privately owned rights. Reference herein to any specific commercial product, process, or service by trade name, trademark, manufacturer, or otherwise does not necessarily constitute or imply its endorsement, recommendation, or favoring by the United States Government or any agency thereof. The views and opinions of authors expressed herein do not necessarily state or reflect those of the United States Government or any agency thereof.

composition of the B-Si particles are characterized by high-resolution and analytical transmission electron microscopy (TEM). We argue on the basis of these results that the metal atoms go exothermically into solution in the B-Si precipitates, and we interpret this propensity in terms of the structural flexibility and electronic properties of the B-Si phase. The measured amount of gettering by the B-Si phase in equilibrium with metal-silicide phase is used to quantify the strength of the gettering. This quantification is then used to predict gettering performance, and comparison is made with conventional internal gettering by SiO_2 precipitates [4].

2. Observation of gettering

Figure 1 shows depth profiles of implanted B and gettered Fe in float-zone Si after the following sequence of treatments: 1) formation of equilibrium Fe_2Si on the back side of the 0.25-mm wafer by Fe ion implantation and annealing [5,6], 2) implantation of B on the front side, and 3) annealing at 1000°C to induce B-Si precipitation and equilibration between the gettering sinks and the Fe silicide. The B profile in Fig. 1(a) exhibits the widely observed [7] central peak and wings that result from transient enhanced diffusion coupled with B-Si precipitation where the B concentration exceeds its solid solubility, about 1×10^{20} cm^{-3} at 1000°C [8]. In Fig. 1(b), where the B concentration is lower, the B remains entirely in solution.

It is apparent from Fig. 1 that the gettering of Fe occured predominantly in the region of B-Si precipitation, with no definitive indication of an association between Fe and the B in solution. (Pairing of substitutional B and interstitial Fe, enhanced by the B-induced Fermi-level shift, would be expected to produce a small amount of gettering from solution during the cooling from 1000°C. This effect has been detected by using SIMS with a higher sensitivity than that employed here [9].) A second significant feature of the gettering behavior, suggested by Fig. 1 and reinforced by plots with linear concentration scales, is that the concentration of gettered Fe varies with depth in direct proportion to the concentration of precipitated B. Consistent with such scaling, the proportionality constant at a given temperature remained nearly the same when the implanted B dose was increase by a factor of 5.

Qualitatively similar gettering by B-Si precipitates was found for Fe at 800, 900, and 1100°C, for Co at 900°C, for Cu at 600, 700, and 800°C, and for Au at 850°C. Gettering by substitutional B was also resolved in several of these cases, but this mechanism was consistently superseded by binding to the precipitate sinks when these were present, and it will not be discussed further here. The gettering strengths of the B-Si precipitates for all of the investigated metals and temperatures will be quantified in Sect. 4.

3. Precipitate characterization and mechanistic interpretation

A bright-field, plan-view TEM image of the B-Si precipitates is shown in Fig. 2(a), and a lattice image of one particle appears in Fig. 2(b). In this specimen the near-surface region was amorphized by Si-ion bombardment before B implantation to reduce the number of defects remaining after annealing, thereby enhancing the visibility of the particles. After B implantation, the sample was vacuum annealed at 1100°C for 1 h. The sample preparation for TEM employed chemical thinning instead of ion milling to avoid amorphization by the sputtering beam. The B-Si particles appear in Fig. 2(a) as dark or light features depending on local contrast conditions; their average size is approximately 10 nm. The lattice image from the particle in Fig. 2(b) exhibits the irregular granularity that is characteristic of the absence of long-range structural order.

The composition of the B-Si precipitates was examined with high-resolution analytical TEM. Using a beam diameter of ~1 nm and samples thicknesses comparable to the precipitate size, the B-to-Si atomic ratio was estimated from electron energy loss spectroscopy (EELS), and the metal-to-Si ratio was determined using energy-dispersive x-ray spectroscopy (EDS). For comparison, EELS analysis was also performed on bulk crystalline B_3Si; this material was synthesized by heating a stoichiometric mixture of B and Si powders at 1250°C {Terry???}, and it was shown by x-ray diffraction and Rutherford backscattering spectrometry to have the equilibrium icosahedral structure and a composition near B_3Si. Results of the EELS analysis are shown in Fig. 3, which includes spectra from a B-Si precipitate in B-implanted Si, from the Si matrix adjacent to the B-Si particle, and from bulk crystalline B_3Si. The close similarities in the

shapes and relative amplitudes of spectral features associated with the B-Si precipitate and the bulk B_3Si indicate that the compositions and local bonding are similar.

Analysis by EDS confirmed the association of gettered Cu atoms with B-Si precipitates. Examination of a B-Si particle yielded a Cu-to-Si ratio on the order of 0.01 {Joe???}, consistent with the amount of gettered Cu, whereas no Cu was detected in the adjacent matrix. Moreover, the strength of the Cu signal was greater for transmission of the electron beam through the center of the precipitate than for transmission through the edge region, suggesting that the metal atoms resided in the bulk of the particle rather than its periphery.

These findings and those of Sect. 2 lead us to two inferences. First, while the B-Si precipitates lack long-range structural order, they are very similar to crystalline B_3Si in local bonding and structure. This is supported by the above EELS measurements. Additionally, it is reinforced by consideration of the effective solubility of B in Si in the presence of the precipitates. The effective B solubility is indicated by the concentration at which the diffusion tails in B profiles such as that in Fig. 1(a) intersect the central precipitation peak. This concentration conforms within experimental uncertainty to the published thermodynamic solubility of B in Si [8], implying a near equality of chemical potentials. Our second inference is that the gettering occurs by exothermic segregation of metal atoms from solution in the Si phase to solution in the B-silicide phase. The above EELS analysis suggests that this is so, and it is also consistent with the aforementioned proportionality between the concentration of gettered metal atoms and the concentration of precipitated B atoms. This interpretation is also plausible on physical grounds, as we now discuss.

The B_3Si unit cell consists of a rhombohedron with icosahedra at the corners and two additional Si atoms along the longer body diagonal [10]. Boron-rich solids with icosahedral bonding have several characteristics that are expected to promote the incorporation of transition-metal atoms, including the strong electron affinity and high stability of the icosahedral units, the presence of relatively large open volumes outside the icosahedra, and the high variability and flexibility of the overall structure and bonding configuration [11,12]. In such a material,

transition metals may serve as electron donors and reside in the interstices with relatively little steric hindrance. Moreover, the structural complexity and the highly refractory character of B-rich solids may account for the absence of fully developed crystallinity in the 10-nm B-Si precipitates formed at 1100°C and below.

4. Quantification of gettering strength

We assessed the strength of metal gettering at the B-Si precipitates by measuring the number of gettered atoms per precipitated B atom in equilibrium with the metal-silicide phase. The method of establishing this equilibrium was described in Sect. 2. The atomic fraction of metal atoms in solution is then equal to the solid solubility in the presence of the metal silicide,

$$C_S[\mathrm{sil}] = \exp(-\Delta G_{\mathrm{sil}}/kT) \tag{1}$$

with

$$\Delta G_{\mathrm{sil}} \equiv \Delta H_{\mathrm{sil}} - T\Delta S_{\mathrm{ex,sil}} \,. \tag{2}$$

Here ΔH_{sil} is the change in enthalpy when one metal atom moves from the silicide phase to solution, and ΔS_{ex} is the excess change in entropy after the configurational contribution due to fractional occupation of multiple solution sites is taken into account separately. The applicability of Eq. (1) to our experimental conditions was confirmed for Fe by using deep-level transient spectroscopy (DLTS) to measure the concentration of unprecipitated Fe in equivalently treated Si lightly and uniformly doped with B [6]. After an equilibration anneal at 950°C and subsequent sectioning to the central region of the wafer, a concentration of $N_{\mathrm{Si}}C_S = 1.1\times10^{14}$ Fe/cm^2 was measured, N_{Si} being the atomic density of Si. This is in satisfactory agreement with the published solubility of $N_{\mathrm{Si}}C_S[\mathrm{sil}] = 1.4\times10^{14}$ Fe/cm^2 at 950°C [2,8].

Pending a more complete understanding of metal-atom incorporation into the B-Si phase, we make the following assumptions in order to parameterize the strength of the gettering effect: 1) the metal atoms occupy pre-existing interstitial sites and saturate at one per site; 2) all sites are equivalent; 3) occupation of one site does not affect the properties of others; and 4) the number of sites is one per electronegative icosahedral unit of B_3Si, or about 0.1 per B atom. The metal atom fraction in solution in equilibrium with the B-Si precipitates is then given by

$$C_S[BSi] = \{\theta/(1-\theta)\} \exp(-\Delta G^*_{BSi} / kT) \quad (3)$$

where θ is the fractional occupation of gettering sites and is taken to be to the number of gettered metal atoms per precipitated B atom divided by 0.1. We add an asterisk to the binding free energy in Eq. (3) to emphasize that it must at present be regarded as an effective rather than a fundamental quantity. Nevertheless, Eq. (3) should provide an empirically valid description of gettering when the sinks are far from saturation. Since $\theta \lesssim 0.2$ for the experiments reported here, with $\theta \lesssim 0.01$ in the important case of Fe, we provisionally take Eq. (3) to be applicable.

As a consistency check on the above interpretation, we examined the variation of $C_S[BSi]$ with θ for Fe. This was done by performing an additional gettering experiment where, in contrast to the procedure described in Sect. 2, Fe silicide was not introduced to stabilize the solution concentration at the solubility; hence, only pre-existing Fe was present in the Si. After a gettering anneal at 1000°C, SIMS profiling showed a decrease in θ from the silicide-buffered experiments of about a factor of 6, while DLTS indicated that the final solution concentration was about one tenth of the published solubility. Considering the experimental uncertainties, this is consistent with the expected proportionality between $C_S[BSi]$ and θ for small θ.

To extract ΔG^*_{BSi} as a function of temperature for Fe, Co, Cu, and Au, we combined Eqs. (1) and (3) by using the equilibrium condition $C_S[sil] = C_S[BSi]$, evaluated θ from our experiments, and from the literature took $\Delta G_{sil}[Fe] = 2.94$ eV – 8.2 kT [2,8], $\Delta G_{sil}[Co] = 2.83$ eV – 7.6 kT [2,8], $\Delta G_{sil}[Cu] = 1.74$ eV – 3.9 kT [13], and $\Delta G_{sil}[Au,850°C] = 2.31$ eV [14]. Results are shown in Fig. 4. The reference state for these effective binding free energies is the mobile metal atom in interstitial solution in the Si lattice. (This definition includes Au, notwithstanding the presence of immobile Au atoms in substitutional sites in the Si lattice [8].)

The variation of the effective binding free energy among the impurity species in Fig. 4 reflects the stabilities of both the solution and the bound states, and this complicates the interpretation of observed trends. We nevertheless speculate that the values for Co and Fe lie above those for Cu because the former elements, with their higher valences, can donate more electrons to the electronegative icosahedral units of the B-Si phase. The relatively large binding

free energy for Au may result from this atom being less readily accommodated in the interstitial solution site of the Si lattice, as is suggested by the preference of Au for substitutional sites [8].

5. Prediction of gettering performance

The effective binding free energies in Fig. 4 are large enough to produce substantial segregation to the sinks at technologically relevant temperatures. Moreover, this segregation should occur regardless of the initial concentration of metal atoms in solution in the Si, in contrast to gettering by silicide precipitation [2-4], which occurs only when the solution is supersaturated. In mathematical terms, this important difference arises from the presence of the factor $\theta/(1-\theta)$ in Eq. (3) and its absence in Eq. (1).

The implications of the above properties for gettering are illustrated in Fig. 5, where we present model calculations for Fe. The diffusion equation with source terms taking account of the interaction of Fe atoms with the gettering sinks was solved numerically [13]. Our treatment assumed that 1×10^{17} B/cm^2 precipitated as spherical B_3Si particles with a diameter of 10 nm, this in a layer centered 5 μm beneath the surface of a wafer with a total thickness of 500 μm. The boundary condition on the solution concentration at the periphery of the particles was assumed to be given by Eq. (3). Plotted in Fig. 5 for several temperatures is the calculated solution concentration at a depth of 1 μm. Included for comparison are model predictions for conventional internal gettering, where SiO_2 particles and related defects within the underlying bulk of Czochralski wafers provide sites for nucleation and growth of $FeSi_2$ precipitates. The parameterization of this latter process conforms to the findings of Ref. 4, with the product of sink density and sink radius being equated to 4.8×10^{15} cm^{-2}. The thickness of the near-surface sink-free zone is taken to be 10 μm.

Figure 5 shows that, in the regime of Fe impurity levels $\lesssim10^{12}$ cm^{-3} that typifies high-quality wafers, gettering by SiB precipitates is potentially more effective than internal gettering. In particular, the impurity concentration in the near-surface device region is reduced more rapidly due to the proximity and large capture cross section of the assembly of B-Si particles. Moreover, the concentration is ultimately reduced to a lower value, even though $\Delta G_{Sil}[Fe] >$

ΔG_{BSi}[Fe], because of the differences between precipitation gettering and segregation gettering embodied in Eqs. (1) and (2); indeed, at 800 and 1000°C where the solubility of Fe exceeds the starting concentration, there is substantial gettering by the B-Si phase and none by internal gettering. (The B-Si precipitates also getter Fe somewhat more effectively than cavities [6], but this is not so for Cu [13].)

The near-surface Fe concentration in the presence of the B-Si sinks is seen in Fig. 5 to go through a pronounced minimum as a function of time at higher temperatures. This reflects the interplay of two opposing trends: the diffusion-limited transfer of Fe from 1 μm to the nearby sinks at short times, and the increase of C_S[BSi] at longer times as the slower acquisition of Fe from the underlying bulk increases θ (see Eq. (3)). This is an effect that might be exploited in device processing. At the lowest temperature of 400°C, the realization of the final surface concentration is delayed from about 10^2 to 10^6 s due to the finite cross section presented by the B-Si particles. Despite the relatively high density of these particles seen in Fig. 2(a), the solution concentration within the implanted layer is predicted not to reach full equilibrium as long as Fe is diffusing inward from the bulk at much higher concentrations.

6. Conclusion

We have shown that B-Si precipitates in Si strongly bind Fe and other transition-metal impurities, providing gettering in the low-impurity regime that is predicted to be superior to internal gettering and also, in the case of Fe, to cavities. While the present investigation dealt with ion-implanted B, the use of B doping during growth to achieve the same end is conceivable, particularly in light of the very high B levels currently grown into p^+ wafers.

Acknowledgments

D. Emin provided key insights into the nature of B-rich phases. Valuable discussions were held with D. J. Eaglesham and J. M. Poate.

References

[1] The National Technology Roadmap for Semiconductors (Semiconductor Industry Assoc., San Jose, California, 1994) pp. 110-131.

[2] W. Schröter, M. Seibt, and D. Gilles, in: Materials Science and Technology, Vol. 4; Electronic Structure and Properties of Semiconductors, ed. W. Schröter (VCH, New York, 1991) pp. 539-589.

[3] K. Graff, Metal Impurities in Silicon-Device Fabrication (Springer-Verlag, Berlin, 1995).

[4] D. Gilles, E. R. Weber, and S.-K. Han, Phys. Rev. Lett. 64 (1990) 196.

[5] X. W. Lin, J. Desimoni, H. Bernas, Z. Liliental-Weber, and J. Washburn, Mater. Res. Soc. Symp. Proc. 320 (1994) 97.

[6] S. M. Myers, G. A. Petersen, and C. H. Seager, J. Appl. Phys., Oct. 1996, in press.

[7] S. Solmi, E. Landi, and F. Baruffaldi, J. Appl. Phys. 68 (1990) 3250.

[8] Properties of Silicon (INSPEC, London, 1988) pp. 430-451.

[9] P. A. Stolk, J. L. Benton, D. J. Eaglesham, D. C. Jacobson, J.-Y. Cheng, J. M. Poate, S. M. Myers, and T. E. Haynes, Appl. Phys. Lett. 68 (1996) 51.

[10] R. W. Olesinski and G. J. Abbaschian, Bull. Alloy Phase Diag. 5 (1984) 478.

[11] D. Emin, Physics Today, January 1987, pp. 55-62.

[12] M. Carrard, D. Emin, and L. Zuppiroli, Phys. Rev. B 51 (1995) 11270.

[13] S. M. Myers and D. M. Follstaedt, J. Appl. Phys. 79 (1996) 1337.

[14] S. M. Myers and G. A. Petersen, Mater. Res. Soc. Symp. Proc. 396 (1996) 733.

Figure captions

1. Depth profiles of implanted B and gettered Fe for B concentrations above (a) and below (b) the solubility. Back-side $FeSi_2$ was formed by implanting 5×10^{16} Fe/cm^2 at 100 keV and 350°C and then vacuum annealing at 520°C for 1 h and at 1000°C for 2 h. Boron was subsequently implanted into the front side at 300 keV and a dose of 2.5×10^{16} cm^{-2} (a) or 2.5×10^{15} cm^{-2} (b), and the specimen was finally annealed for 2 h at 1000°C.
2. Bright-field plan-view TEM image (a) and [110] Si lattice image (b) of B-Si precipitates in Si. The specimen was first amorphized by implanting 1×10^{16} Si/cm^2 at 180 keV, 5×10^{15} Si/cm^2 at 100 keV, and 5×10^{15} Si/cm^2 at 50 keV. Boron was then implanted at 50 keV to a dose of 5×10^{16} cm^{-2}, and the sample was finally anneal at 1100°C for 2 h.

3. EELS spectra from a B-Si precipitate, from the adjacent Si host matrix, and from bulk crystalline B_3Si. The Si specimen is that of Fig. 2.
4. Binding free energies of metal atoms in the B-Si phase relative to interstitial solution in Si.
5. Predicted solution concentration in the near-surface region of a Si wafer resulting from gettering by B-Si precipitates or from conventional internal gettering by SiO_2 precipitates.

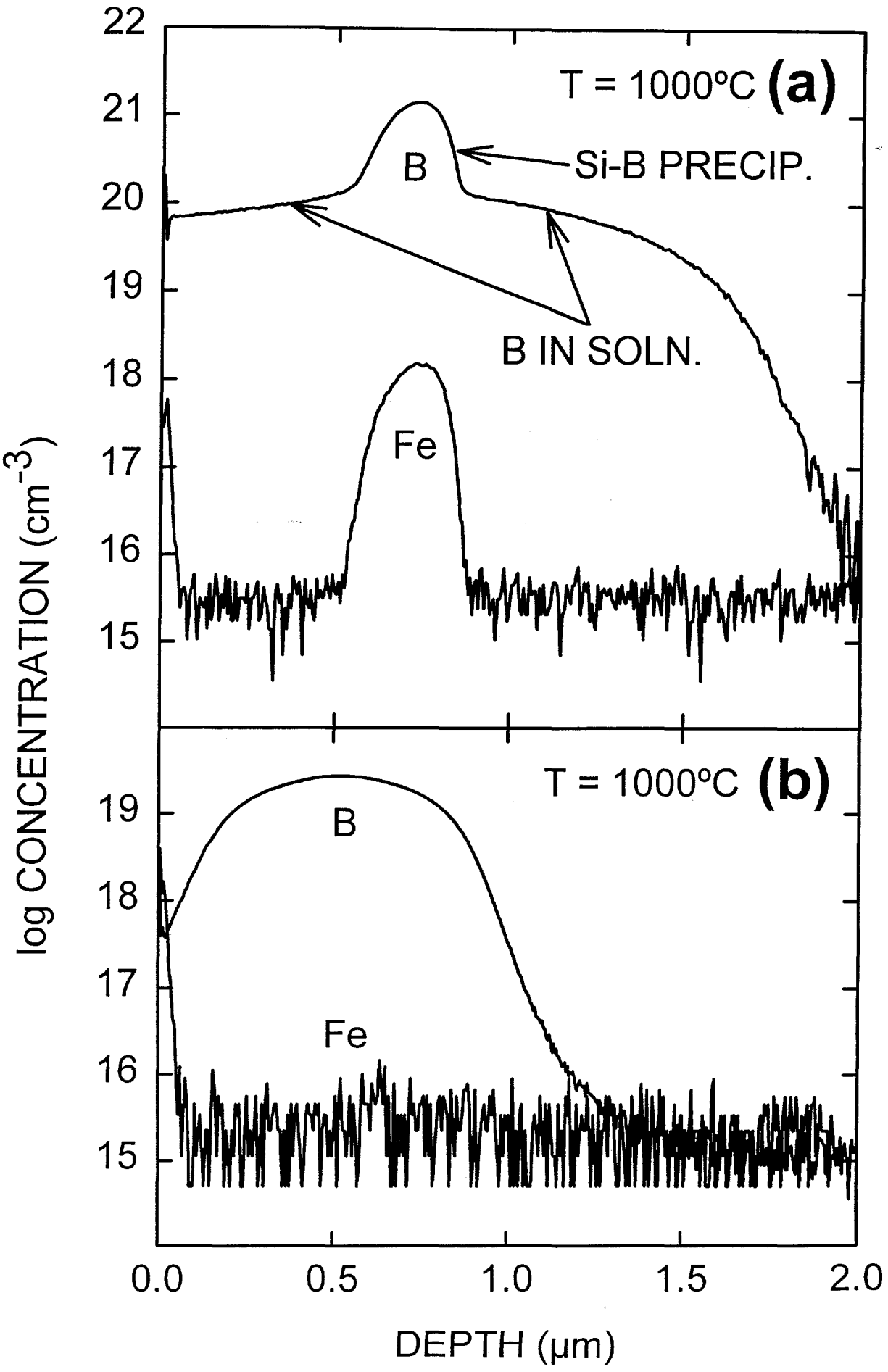
T = 1000°C (a)
B
Si-B PRECIP.
B IN SOLN.
Fe
T = 1000°C (b)
B
Fe
log CONCENTRATION (cm-3)
22
21
20
19
18
17
16
15
19
18
17
16
15
0.0
0.5
1.0
1.5
2.0
DEPTH (μm)

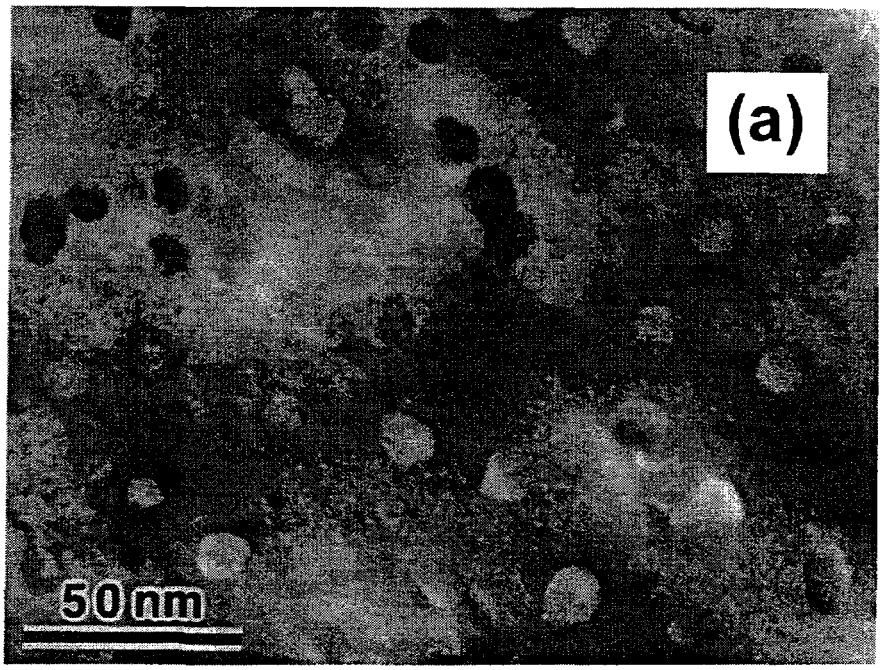
(a)
50nm

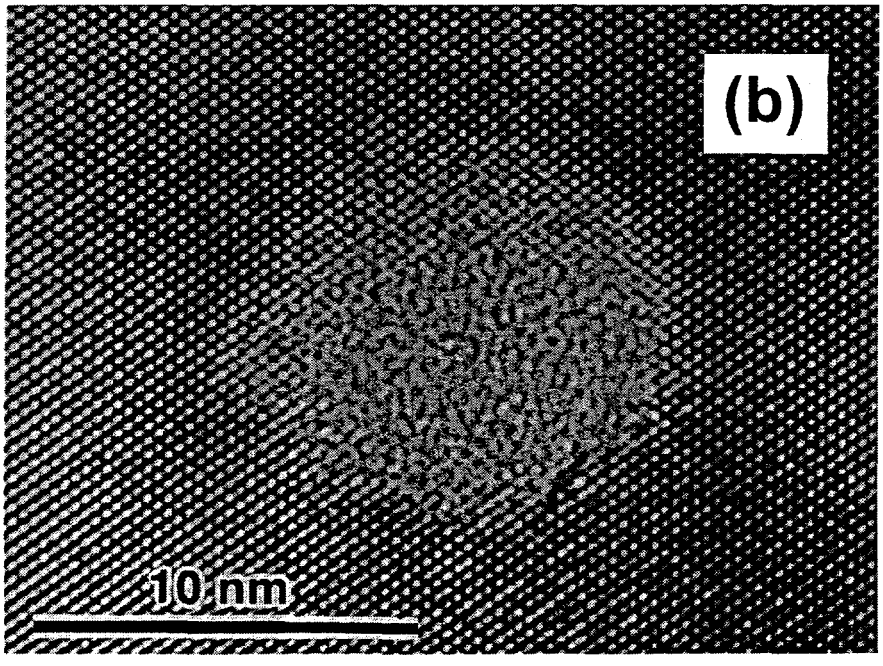
(b)
10 nm

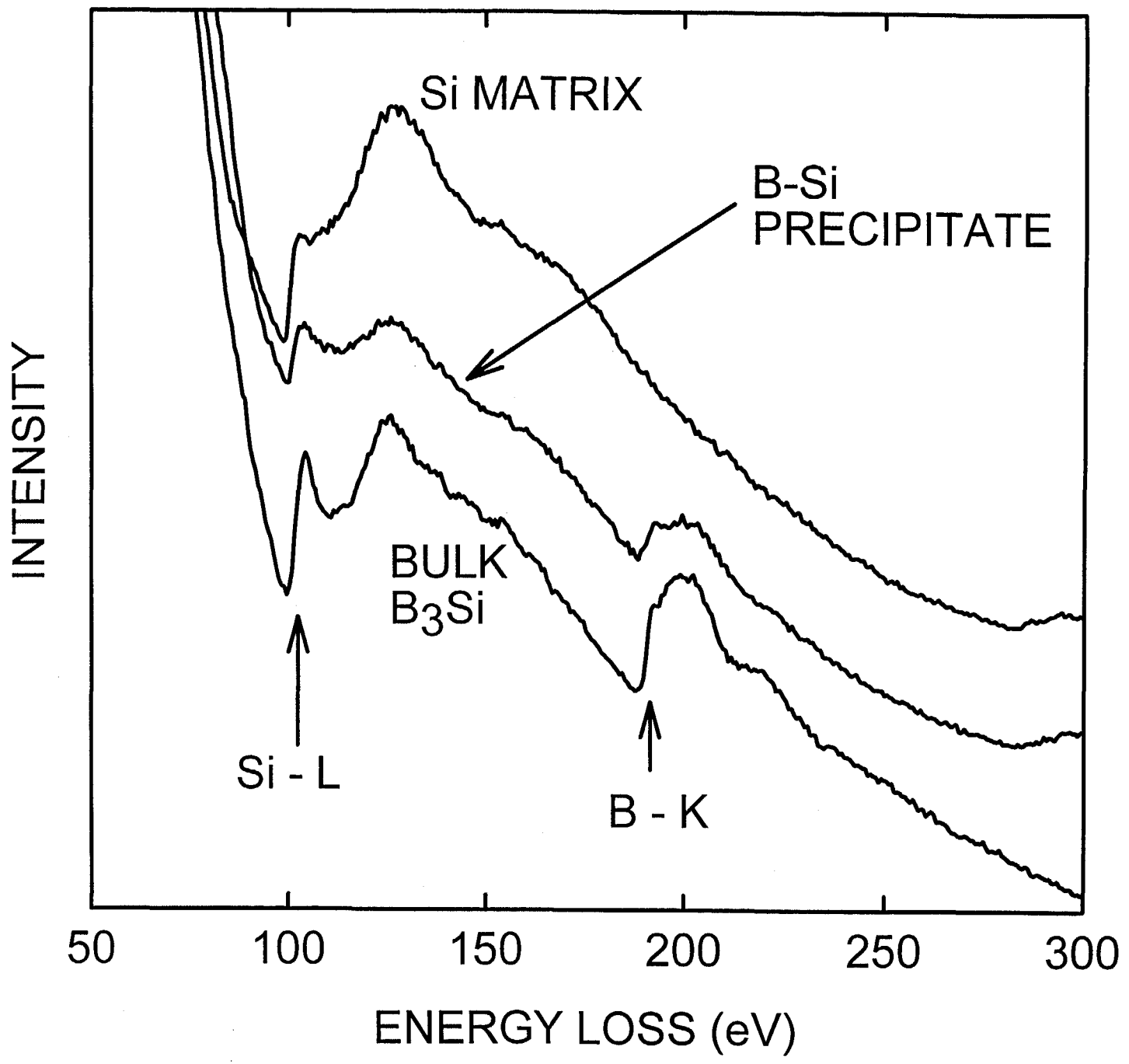
Si MATRIX
B-Si
PRECIPITATE
BULK
B_3Si
Si - L
B - K
INTENSITY
50
100
150
200
250
300
ENERGY LOSS (eV)

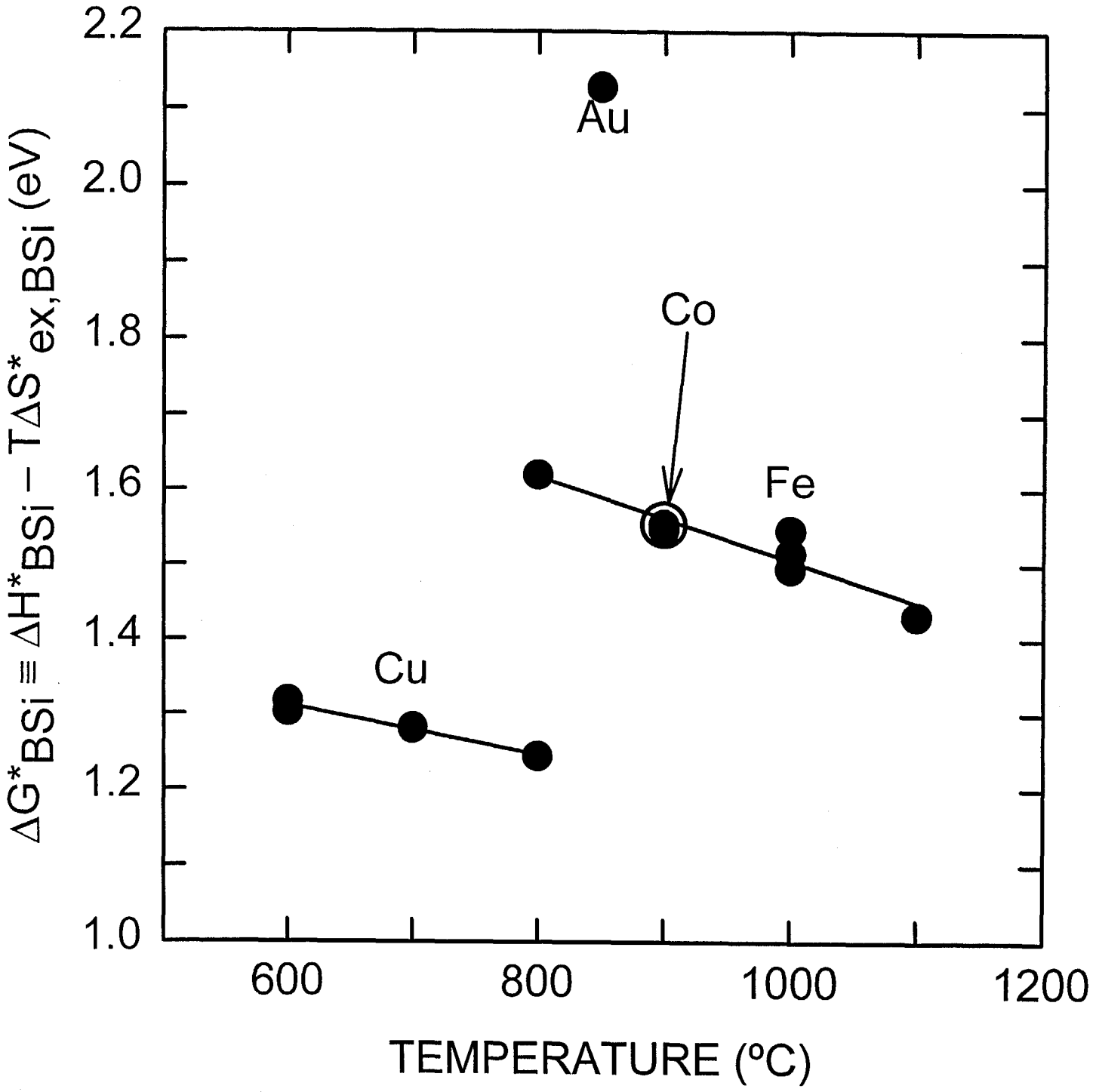
2.2
2.0
1.8
1.6
1.4
1.2
1.0
Au
Co
Fe
Cu
600
800
1000
1200
TEMPERATURE (°C)
ΔG*BSi ≡ ΔH*BSi – TΔS*ex,BSi (eV)

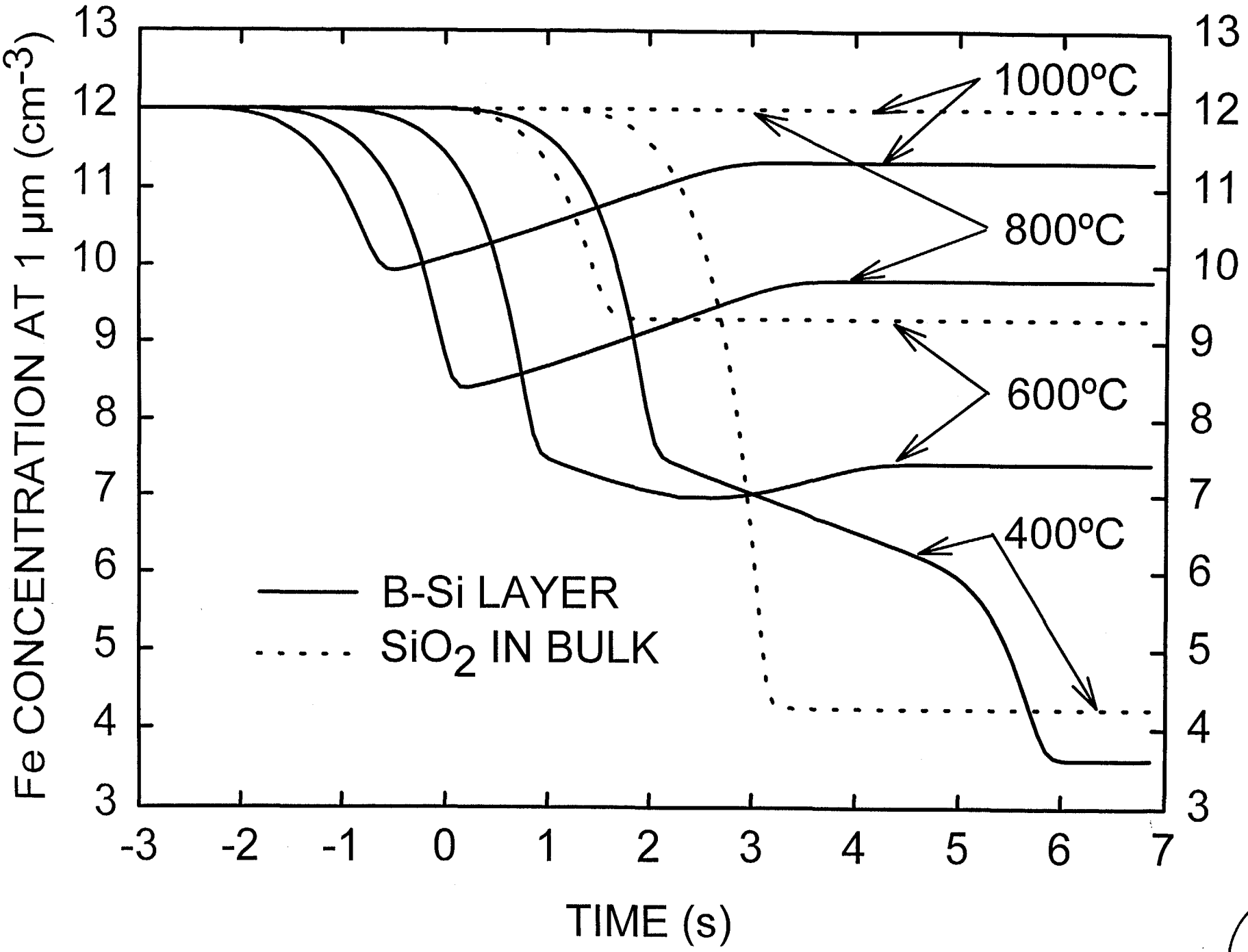
Fe CONCENTRATION AT 1 µm (cm-3)
TIME (s)
1000°C
800°C
600°C
400°C
B-Si LAYER
SiO2 IN BULK
13
12
11
10
9
8
7
6
5
4
3
-3
-2
-1
0
1
2
3
4
5
6
7